BEAM SIMULATION CODE USING ACCURATE GAP FIELD DISTRIBUTIONS IN A DRIFT TUBE LINAC

Takao Kato

KEK, National Laboratory for High Energy Physics

1-1 Oho-cho, Tsukuba-shi, Ibaraki-ken 305, Japan

Abstract

A beam simulation code, LINSAC (Linac Simulation Code with an Accurate Field Distribution), was recently developed in order to simulate a high-intensity beam in a drift tube linac (DTL). A step-by-step calculation within a unit cell is performed on the basis of the exact longitudinal and transverse electric field distributions in the drift tube gap. The code takes into account the particle-to-particle (P-P) electric forces among all particles for a space-charge calculation. An outline of the code is given. Some calculated results concerning both the beam behavior in a drift-tube unit cell and that in a low-energy part of the DTL planned for the JHP 1-GeV proton linac are also described. An indication of beam halo formation due to intrabeam scattering is discussed.

Introduction

In the PARMILA code, the average accelerating field over the unit cell is taken into account, which is usually supplied by a SUPERFISH calculation in terms of the transit time factor and the average accelerating field. The code has been proved to have a sufficient accuracy for calculating the geometry of a drift tube linac, that is determined, in principle, by the particle motion on a stable rf phase along the beam axis. The reasons for the accuracy mentioned above are partly due to the fact that the test particle travels along the center axis of the linac, where there is neither focusing nor defocusing electromagnetic fields, and partly due to single-particle motion without any space-charge effects. Once a multi-particle beam simulation of a high-intensity beam is attempted, two problems are introduced. One arises from space-charge effects; the other arises from the using the average electric fields. In the PARMILA code, all of the forces on a particle are averaged over some rather long period (for example, a unit-cell length) on the assumption that the instantaneous location of a particle related to both of the other particles and the accelerating structure has a negligible effect. However, it can be said that the accuracy of the approximation becomes worse as the variation in the particle's motion during the averaging period becomes large. Therefore, a beam simulation code, named LINSAC (Linac Simulation Code with an Accurate Field Distribution), has been developed in order to simulate a high-intensity beam in a DTL. A step-by-step calculation within a unit cell is performed on the basis of the exact longitudinal and transverse electric field distributions in a drift tube gap. The code takes into account the particle-to-particle (P-P) electric forces among all of the particles for the space-charge calculation. The code is highly vectorized up to a vectorized ratio of more than 99.7% in order to make the best use of the supercomputer, HITAC S820/80. A typical calculation time for a 45-cell simulation (2000 particles and 180 steps per rf period) is 24 minutes. In this paper, an outline of the code is given. Some of the calculated results for a low-energy part of the DTL planned for the 1-GeV proton linac in JHP[1] are also given. An indication of beam halo formation due to intrabeam scattering is discussed.

Method of calculation

The motion of a particle in an electromagnetic field is written as:

$$\frac{d\mathbf{p}}{dt} = q(\mathbf{E} + \mathbf{v} \times \mathbf{B}), \tag{1}$$

$$\mathbf{p} = m_0 \gamma \mathbf{v},$$

where p is the momentum, q a unit charge, E the electric field, B the magnetic field, m_0 the rest mass, γ the Lorentz contraction factor, and v the velocity of the particle ($v^2 = v_x^2 + v_y^2 + v_z^2$). In the first place, the accelerating field distribution (E_z) along the beam axis in a unit cell is obtained by using the SUPERFISH code. Then, the shape of the field distribution is approximated using a ninth-order polynomial formula. Next, a table of the coefficients of the formula are read into the code. The intensities of the average accelerating fields are normalized to the design value by integrating the axial field within a unit cell. The number of geometries of the drift tube, corresponding to the various particle energies, are required in order to achieve an accurate approximation for all cells of the linac, since the shape of the field distribution gradually varies along with the particle energy.

Next, the electric fields are expanded as a Fourier series using the geometrical period of a unit cell length in order to calculate the radial electric field (E_r) from the accelerating one along the axis. The fields are expressed by:

$$E_z = \sum_{m=0}^{\infty} A_m I_0(k_m r) \cos\frac{2m\pi z}{L} \cos\omega t,$$

$$E_r = \sum_{m=1}^{\infty} \frac{A_m 2m\pi}{k_m L} I_1(k_m r) \sin\frac{2m\pi z}{L} \cos\omega t, \text{ and}$$

$$k_m^2 = \left(\frac{2\pi}{\lambda}\right)^2 \left(\left(\frac{m\lambda}{L}\right)^2 - 1\right),$$

where I_0 and I_1 denote the modified Bessel functions, L the unit cell length, ω the angular resonant frequency, t the time, and λ the free-space wavelength. After calculating the Fourier coefficients (A_m's) using the accelerating field distribution along the axis up to order five, the transverse fields, except for both the time and radial-dependent terms, are calculated. Figure 1 shows the field distributions obtained by a SUPERFISH calculation, and that calculated approximately in the LINSAC at an energy of 3 MeV. Although the azimuthal magnetic fields are also
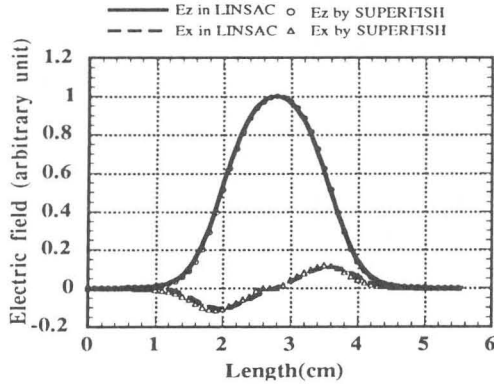
Fig.1 Field distributions in the unit cell used in the LINSAC code.

Fig.2 Change in the transverse energies through the cell vs. the average transverse coordinates for both transverse directions (B'=0).

Fig.3 Change in the transverse kinetic energies through the cell vs. the average transverse coordinates when the magnetic gradient is turned on.

calculated in the code, they are usually set zero, since its contribution is small in the low-energy part of the proton linac.

The other DTL parameters required for the simulation are supplied from the output of the PARMILA code: the unit cell length, length and strength of the quadrupole magnet, length of the drift tube, the stable particle energy and phase, the average accelerating field strength, and the resonant frequency.

Equation (1) can be solved numerically by the Runge-Kutta method of fourth order with a sufficiently small divided timestep. The space-charge force on the i-th particle is taken into account in each timestep of the calculation as a sum of the Coulomb forces calculated from all other particles. It is written as:

$$\mathbf{E}_i = \frac{q}{4\pi\varepsilon_0} \sum_{j \neq i} \frac{1}{\mathbf{r}_{ij}^2},$$

where ε_0 is the permittivity of free space and $\mathbf{r}_{ij}$ is the distance between the i-th and j-th particles. In order to achieve a high vectorized ratio, the unit cell length is divided longitudinally into small step sizes determined by the unit cell length divided by the number of timesteps before the beginning of the main simulation. The electric and magnetic fields in the step are previously assigned and tabulated for all of the cells.

Motion in a unit cell

A test simulation was performed using the JHP DTL (432 MHz) with a randomly distributed beam of 1600 particles having the same magnitude of phase spread as a 3-MeV RFQ output beam. At first, the motion in a unit cell (No.11; from the center of the quadrupole magnet to that of the next one, where the injection energy is 4.26 MeV, the accelerating field is 3 MV/m and the cell length is 6.64 cm), is analyzed.

1)Transverse motion (the current is set to zero)

Figure 2 shows the change in the transverse kinetic energies through the cell as a function of the transverse coordinates when the quadrupole magnet gradient (B') is set to zero, indicating the rf defocusing effects. If the magnetic gradient is turned on (~175 T/m), the transverse kinetic energies vary large on the order of 0.5 keV, reflecting the beginning of the trans-

verse oscillation (Fig. 3). In this case, a change in the transverse kinetic energies arises from the external focusing force combined with the effect of the rf defocusing force.
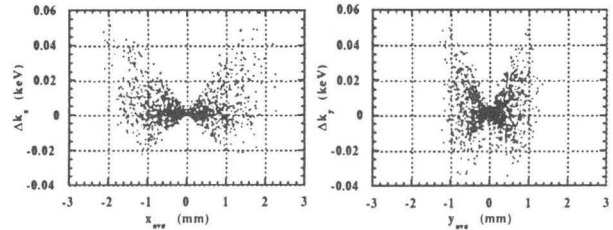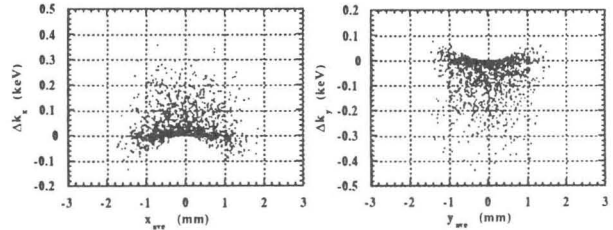
2) Collision (intrabeam scattering)

Figure 4 shows a collision example, in which mainly the transverse kinetic parameters changes. Another collision example is given in Fig. 5-a, showing the longitudinal kinetic energy variation due to acceleration through the initial two cells for two collision particles among 1600 particles. They collide almost longitudinally at a length of 107 mm. Figure 5-b is a magnified plot of (a). In this case, the magnitude of the energy change is not very small, compared with that of the longitudinal oscillation. In conclusion, the collision, which results in large changes of the kinetic parameters, influences the beam quality. However, due to the small Lorentz-contraction factor in a low-energy proton linac, the change in the longitudinal kinetic energy is not sufficiently large to be seen in an electron storage ring.

Results of the DTL simulation

In the beam simulations discussed below, the following beam characteristics were additionally assumed. A random distribution on six-dimensional phase space was assumed for the initial 2000 particles. The values of the transverse twiss parameters of the matched beam were equal to those of the zero-current acceptance of the linac, while those of the mismatched beam were equal to those of the RFQ output beam. The simulations were performed for a low-energy part (45 cells, 11 MeV) of the JHP DTL. The calculated emittance growth is listed in Table 1 as a function of the beam current. The results obtained using PARMILA are also shown. It can be said that the LINSAC code is more sensitive to such parameters as the current and beam matching. It can also be said that the spreads (full width)
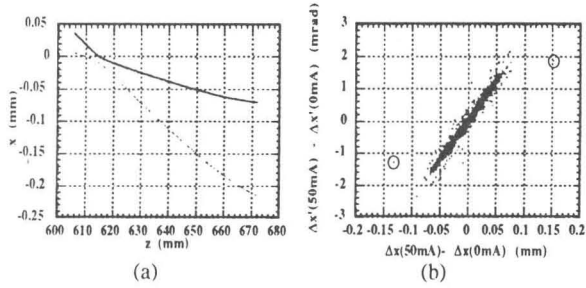
Fig.4 (a) Trajectories (x vs. z) of two collision particles through the eleventh cell. (b) Difference between the change in the x-gradient for a 50-mA beam within the eleventh cell and that for a 0-mA beam as a function of the difference in corresponding x-coordinates. The two circles indicate the collision particles.
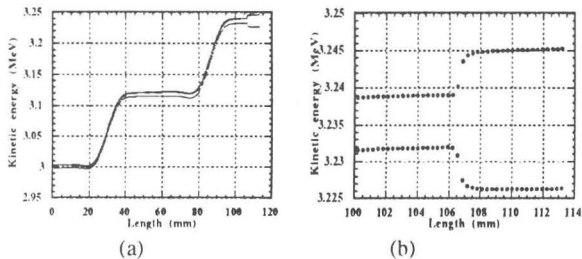
Fig.5 (a) Longitudinal energy variation through the initial two cells for two particles. A change in the energy due to a collision can be seen at a length of 107 mm. (b) A magnified plot of (a).
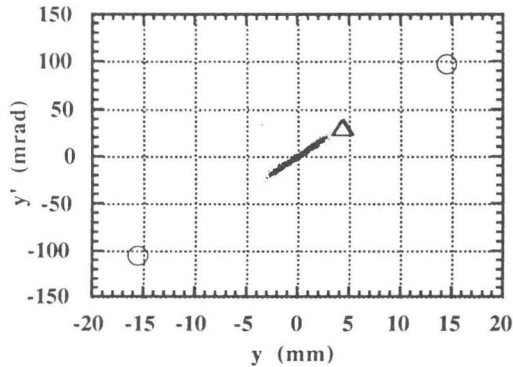
(a)
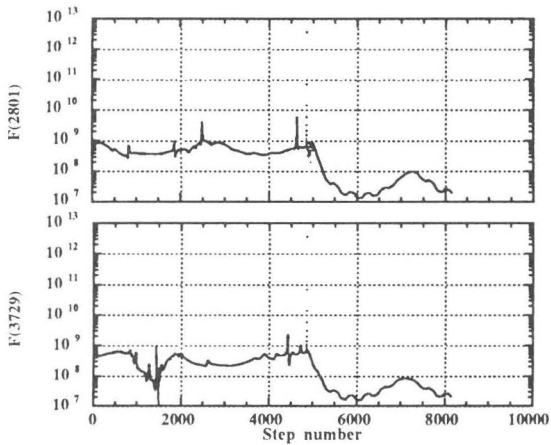
(b)

Table 1 Emittance growth(%) for the matched and mismatched beams vs. the beam current.

LINSAC results (matched/mismatched)

	x(rms)	x(90%)	y(rms)	y(90%)
20 mA	0.8/1.6	1.5/5.2	1.2/3.5	4.6/6.8
50 mA	-0.1/11	2.1/13	0.8/3.5	2.3/8.8
100mA	7.3/39	13/42	9.8/28	16/30

PARMILA results (matched/mismatched)

	x(rms)	x(90%)	y(rms)	y(90%)
20 mA	0/0	1.4/4.0	2.1/0	2.6/0.4
50 mA	2.1/2.5	3.3/5.3	2.5/1.3	3.9/2.4
100mA	2.5/12	5.2/9.0	4.2/3.3	4.4/6.7

of the output beam in both longitudinal and transverse directions by LINSAC simulation are larger than those of PARMILA.

Indication of halo formation

A further simulation was performed using a 100-mA beam of 5000 particles. Figure 6-a shows the output- beam emittances. The circles indicate the two-collision particles, colliding at a step number of around 4858 in the 27-th cell. They should have been lost if the simulation were carried out under the beam-loss conditions, since their y-coordinates are larger than the bore-radius. The coulomb forces in all of the steps for the two particles are shown in Fig.6-b. Figure 6-c shows the typical coulomb forces in a step for all of the particles.They suggest that the collision with such a large Coulomb force mentioned above occurs at rare intervals, and that several pairs happen to collide in a step. Thus, it can be said that all of the collision particles are not always lost. As a result, two or three lost particles among 5000 particls is sufficient in order to explain some parts of the beam halo.

Reference

[1] Y. Yamazaki et al., Proc. Advanced Hadron Facility Accelerator Design Workshop, 1988, Los Alamos, LA-11432-C, p.80, KEK Preprint 87-159, Yamazaki et al., Proc. 1988 Linear Acc. Conf., 79 (1988).

Acknowledgments

(a)

(b)
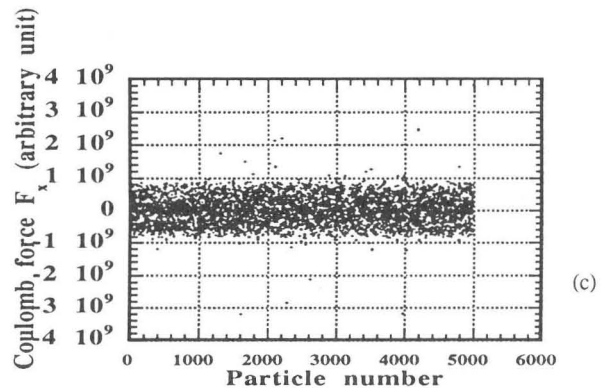
(c)

Fig.6 (a) Output beam emittance (y-y'). The two circles indicate the collision particles in the 27-th cell. (b) Coulomb force (arbitrary unit) for two collision particles in all steps. (c) Coulomb forces in the x-direction in the 2924-th step for all particles.